New developments in ultrasound-modulated optical tomography made by heterodyne holography

A. Brodoline, D. Donnarumma, Michel Gross

▶ To cite this version:

A. Brodoline, D. Donnarumma, Michel Gross. New developments in ultrasound-modulated optical tomography made by heterodyne holography. Digital Holography and Three-Dimensional Imaging 2016, Jul 2016, Heidelberg, Germany. pp.DT1E.3, 10.1364/dh.2016.dt1e.3 . hal-01927325

New developments in ultrasound-modulated optical tomography made by heterodyne holography

A. Brodoline, D. Donnarumma and M. Gross

Laboratoire Charles Coulomb - UMR 5221 CNRS-UM2 Universitée Montpellier Place Eugène Bataillon 34095
Montpellier, France
michel.gross@univ-montp2.fr

Abstract: Ultrasound-modulated optical tomography (UOT) is a technique that combines light and ultrasound able to image deep inside scattering media. A pulsed version of technique involving holography is proposed and discussed.

Ultrasound-modulated optical tomography (UOT) [1] also called acousto-optic imaging [2] is a technique that combines light and ultrasound able to image deep inside scattering media . The ultimate goal of the technique is breast cancer imaging. Heterodyne holography combined with UOT is a powerful tool to detect the UOT tagged photons. Previous experiments are made with phantom samples. Since the sample does not move, the phase of the field remains correlated. Holographic detection is then efficient and shot noise sensitivity is reached [3]. To perform imaging with breast, a new setup with light and ultrasound pulses is proposed. Numerical simulations, that fits with the results of previous work, are made to extrapolate the phantom results to breast imaging with the new setup. They show that breast tumor imaging is possible.
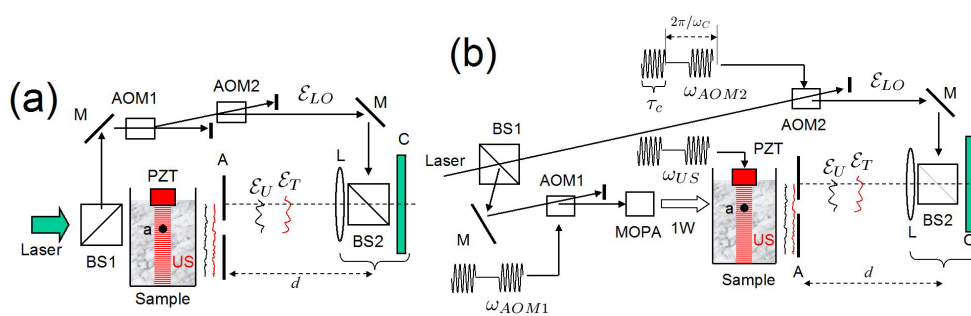

Fig. 1. Typical UOT setup (a) and pulsed modified setup to detect signal whose phase correlation is short (b). BS1, BS2: beam splitter; M: mirror; AOM1,AOM2: acousto optic modulator; PZT: piezoelectric transducer that generates the ultrasonic beam US; a: absorber imbedded in the diffusing sample; A: rectangular aperture; L: lens of focal d; C: camera; $\mathcal{E}_{LO}, \mathcal{E}_T, \mathcal{E}_U$: LO, tagged and untagged fields.

Figure 1 (a) shows the heterodyne holography UOT setup of the phantom experiment [3]. The main laser beam L (frequency ω_L) is split by the beam splitter BS1 into a local oscillator (LO), and a signal beam that is scattered by the diffusing sample. The sample is explored by an ultrasonic (US) beam of frequency ω_{US} generated by a piezoelectric

transducer (PZT). The light transmitted by the sample exhibit to components. The first component (field $\mathscr{E}_T$, frequency $\omega_L + \omega_{US}$) is weak, and corresponds to the photons that have interacted with the US beam and that are tagged by it. The second component (field $\mathscr{E}_U$, frequency ω_L) is the main one. It corresponds to untagged photons, which have not interacted with the US beam. The LO and signal beams are recombined by BS2 onto camera C, which record sequence of frames corresponding to the interference pattern of the two beams.
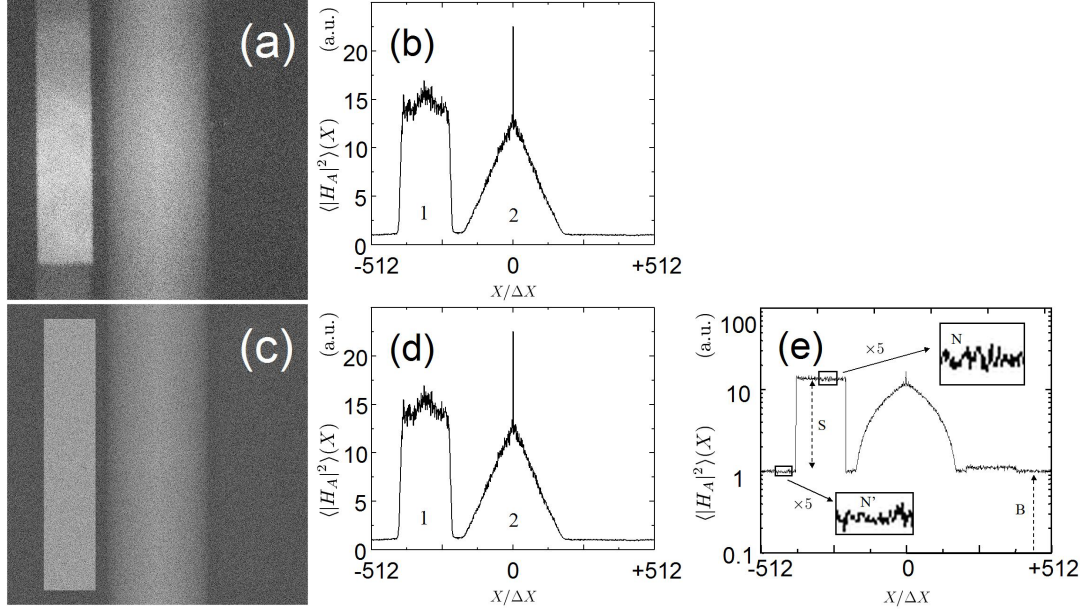

Fig. 2. (a,c) Holographic reconstructed images $|H_A(x,y)|^2$ in plane A. (b,d) Curve $\langle|H_A|^2\rangle(x)$ plotted as function of the y coordinate. Images and curve are calculated from experimental data (a,b) and from simulation (c,d). (e) same as (d) but plotted in logarithmic scale.

To detect selectively the tagged photons, the LO beam frequency is adjusted to $\omega_{LO} = \omega_L + \omega_{US} + \omega_C/4$, where ω_C is the camera frame frequency. Four phase holograms H are calculated from sequences of consecutive frames, and holographic images H_A of the aperture A, back illuminated by the tagged photon, are calculated. Figure 2 (a) shows the reconstructed image $|H_A|^2$ obtained with a sequence of 12 frames, and with a phantom sample, which remains coherent for the whole sequence [2, 3]. The tagged photon signal corresponds to the rectangular bright zone in the left hand side of the image. To better extract the tagged photon signal, $|H_A(x,y)|^2$ is averaged over the y axis yielding $\langle|H_A|^2\rangle(x)$, which is plotted on Fig.2(b). The tagged photon signal corresponds to the rectangular wall 1, which is about $15\times$ higher that the ground floor, which corresponds to shot noise. This means that the tagged photon signal corresponds to an average energy of 15 photo electron per pixel and per mode, for the whole sequence of 12 frames. The triangular peak, in the center of Fig.2 (b) corresponds to a parasitic detection of the untagged photons.

We have performed a simulation of the Fig. 2 (a,b) experiment. The calculation was done in several steps. We assume first that the tagged and untagged speckle fields are known. These fields, which are random, are calculated within aperture A. We calculate then the tagged and untagged fields in the camera plane by holographic reconstruction. We assume then that the LO field, which is flat field, is known. We calculate the intensity corresponding to the sum of the tagged, untagged and LO fields on each pixel of the camera, and we convert the optical signal into photo electrons. Since shot noise is the dominant noise in holographic experiments, we added to the photo electron signal of each frame and each pixel, a random noise corresponding to shot noise,

We consider all frames of the sequence, and we calculate the hologram H of the light scattered by the sample. We propagate H from the camera plane C to the aperture plane A yielding hologram H_A. We selected within H_A the tagged photon signal and to calculate its weight. Note that the data analysis made with the frame simulation is the same as in ref. [3] experiment. The results of simulation are presented in Fig.2(c) and (d) for the images $|H_A(x,y)|^2$, and for the curve $\langle|H_A|^2\rangle(x)$. Agreement validate our simulation.

We have plot $\langle|H_A|^2\rangle(x)$ in logarithmic scale in Fig. 2(e). To extract the tagged photon signal, one has to subtract the noise background from the tagged photon signal, and to average on the pixels located within aperture A. One has thus

to consider the signal S (see Fig. 2 (e)) and the background noise B. We have here $S/B \simeq 15 - 1 = 14$. On the other hand, the noise on signal N is much lower than B. Since the background is a random speckle, N is roughly equal to B divided by the square root of the number of pixels used in averaging.
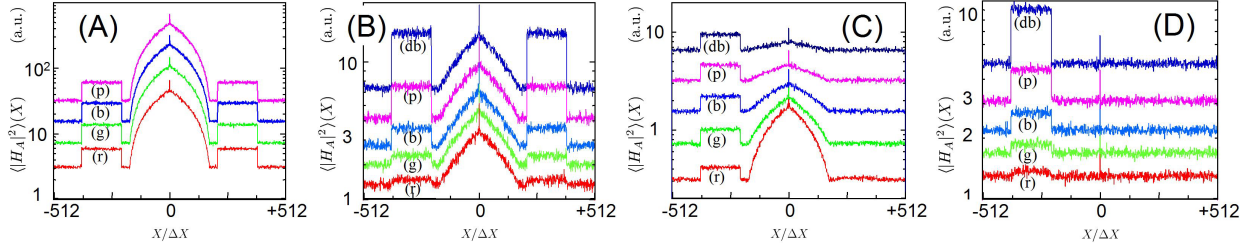

Fig. 3. Curve $\langle |H_A|^2 \rangle (x)$ obtained by simulation with regular (A,B) and lock-in camera (C,D).

To detect the tagged photon of a sample whose decorrelation time τ_c is short: $\tau_c = 0.1$ ms for breast in vivo [4], we propose to use a UOT heterodyne setup, in which the LO, signal and US beams are synchronously pulsed (see Fig. 1 (b)). To evaluate the performances of the pulsed setup, we have performed simulations by considering either a regular camera, or a lock-in cameras, similar to the ones recently developed [5–7] or commercially available (*e.g.* heliCam™ C3, Heliotis). For the regular camera, we have considered an exposure time τ_c, and a frame time interval $2\pi/\omega_C$ larger than τ_c: the correlation of the fields is lost from one frame to the next. For the lock-in camera, we have considered a recording time $\tau_C = 2\pi M/\omega_C$, where M is the number of frames: the correlation is conserved.

Figure 3 shows the curves $\langle |H_A|^2 \rangle (x)$ obtained in simulation with a regular (A,B) and a lock-in camera (B,C). The LO energy is 10^4 per frame, and plots are made in logarithmic scale. Consider Fig. 3 (A,C) calculated with a tagged photon energy of 1 photo electron per mode and per τ_c with for the regular (A) and the lock-in (C) camera. The curves are calculated with M frames: $M = 4$ (r), 8 (g), 16 (b), 32 (p) and 64 (db). For both camera types, the height S of the tagged photon signal the same. Moreover, the signal versus background ratio S/B does not depend on M and is about 1. The curves of Fig. 3 (B,D) are calculated for the regular camera with $M = 4$ (B), and for the lock-in camera with $M = 64$ (D), by decreasing the tagged photon signal from 1 photo electron per τ_c (db) downtown 1/16 (r). For the same tagged photon energy in photo electron per τ_c, the tagged photon signal S is the same for the regular (B) and the lock-in (D) camera.

The results presented here show that pulsed heterodyne holography UOT should be used for breast imaging. Indeed, consider a diffusing sample of thickness $l = 3$ cm, whose diffusion coefficient is $\mu' = 1$ mm^{-1}. The light transmitted by the sample is a speckle pattern that covers an area $S \sim h^2$ in the sample outgoing plane, and that emits light in $N_m = 2\pi S/\lambda^2 = 8.8 \ 10^9$ modes. On the other hand, the sample average transmission is $T = 1/(\mu' l) = 3 \ 10^{-2}$, if one neglects absorption, and is about 10 times lower for low absorption: $T = 3 \ 10^{-3}$. For a quantum efficiency $Q = 0.3$, the camera sees, without and with absorption, $N_p T Q/N_m = 400$ and 40 untagged photo electrons per mode and per τ_c, and 0.4 and 0.04 tagged photo electron. By averaging the background of 1 photo electron per mode and per τ_c over the $\sim 10^5$ pixels (or modes) of the image of the aperture, the expected noise is $1/\sqrt{10^5} = 1/300$. This figure is much lower than the tagged photon signal: 0.4 and 0.04.

References

1. Daniel S Elson, Rui Li, Christopher Dunsby, Robert Eckersley, and Meng-Xing Tang. Ultrasound-mediated optical tomography: a review of current methods. *Interface Focus*, 1(4):632–648, 2011.
2. Steffen G Resink, Albert C Boccara, and Wiendelt Steenbergen. State-of-the art of acousto-optic sensing and imaging of turbid media. *Journal of biomedical optics*, 17(4):0409011–04090110, 2012.
3. Michel Gross, Philippe Goy, and Mohamed Al-Koussa. Shot-noise detection of ultrasound-tagged photons in ultrasound-modulated optical imaging. *Optics letters*, 28(24):2482–2484, 2003.
4. M Gross, P Goy, BC Forget, M Atlan, F Ramaz, AC Boccara, and AK Dunn. Heterodyne detection of multiply scattered monochromatic light with a multipixel detector. *Optics letters*, 30(11):1357–1359, 2005.

5. Akira Kimachi. Real-time heterodyne speckle pattern interferometry using the correlation image sensor. *Applied optics*, 49(35):6808–6815, 2010.

6. Rikesh Patel, Samuel Achamfuo-Yeboah, Roger Light, and Matt Clark. Widefield heterodyne interferometry using a custom cmos modulated light camera. *Optics express*, 19(24):24546–24556, 2011.

7. Kinia Barjean, Kevin Contreras, Jean-Baptiste Laudereau, Éric Tinet, Dominique Ettori, François Ramaz, and Jean-Michel Tualle. Fourier transform acousto-optic imaging with a custom-designed cmos smart-pixels array. *Optics letters*, 40(5):705–708, 2015.